

***Cortical Thickness Measurement of Parkinson's Disease Patients and  
Healthy Controls by using the Hildebrand & Rügsegger Method***

***Sahand Talai, B.Sc.  
Supervisor: Nils Daniel Forkert, PhD***

***BMEN 619  
Final Project Report  
April 2016***

## I. Introduction

Parkinson's disease (PD), the second most common progressive neurodegenerative disease after Alzheimer's disease (AD), is characterized by a range of motor and non-motor symptoms. Predominant motor symptoms include, resting tremor, rigidity, postural instability and bradykinesia, whereas, olfactory dysfunction, sleep disorder, autonomic and cognitive dysfunction are the main non-motor related symptoms<sup>1</sup>. PD can be categorized into idiopathic Parkinsonian disease (IPD) and atypical Parkinsonian syndromes, which include progressive supranuclear palsy (PSP), multiple system atrophy (MSA), and corticobasal degeneration (CBD). The underlying physiological causes of IPD is still debated, however, it is widely accepted that IPD is mainly associated with a progressive neuronal loss in pars compacta of substantia nigra (SN) and also in other pigmented nuclei<sup>2</sup> followed by white matter (WM) vitiation<sup>3,4</sup>. In PSP, midbrain atrophy along with the widening of the third ventricular and tegmental atrophy are observed<sup>5</sup>. In midbrain atrophy anteroposterior midbrain diameter is reduced and an abnormal superior profile which consists of a flat or concave compared to a convex in healthy controls is observed<sup>6</sup>. The predominant neurological changes in PSP consists of neuronal loss and gliosis in the globus pallidus and substantia nigra<sup>7</sup>. As of now, there are no clinical procedures to stop PD progression. However, some common therapies to slow down disease progression or mitigate the symptoms include medication, cell transplantation, and deep brain stimulation<sup>8</sup>. Parkinson's disease diagnosis is commonly conducted by symptom monitoring along with criteria defined by the UK Parkinson's Disease Society Brain Bank<sup>9</sup>, the US National Institute of Neurological Disorders and stroke<sup>9</sup> and the Unified Parkinson's Disease Rating Scale<sup>10</sup> (UPDRS). Moreover, several methods for the image-based classification of IPD and PSP patients have been proposed in the past. Within this context, high-resolution T1-weighted MRI datasets have been used for classifying IPD and PSP patient based on atrophy-related differences in regional brain volumes<sup>11</sup>. Other studies have shown that positron emission tomography<sup>12</sup>, as well as T2\*<sup>13</sup> and susceptibility-weighted imaging (SWI)<sup>14</sup> MRI datasets are also useful to differentiate IPD and PSP patients based on differences regarding the regional brain iron metabolism or local brain iron accumulation. Furthermore, several studies have shown a slight reduction in cortical thickness and volume in IPD compared to healthy controls (HC)<sup>6</sup>. The cerebral cortex, which consists of highly folded sheets of neuron, has thickness values ranging between 1 and 4.5 millimeters<sup>15</sup>. The importance of studying the cortex in neurodegenerative and psychiatric diseases is that regionally specific cortical thinning is an effective biomarker for identifying causative factors of the illness. For instance, irregular thick or thin cortex may be related to changes in gray matter which is correlated with illness such as Parkinson's disease or schizophrenia. Therefore, image based and post mortem studies have been conducted to quantify the thickness of this structure. Thickness in primitive and homogenous geometrical shapes such as spheres and plates are intuitively well defined and understood. However, inhomogeneous anatomical structures such as the cortex require a broader and more inclusive definition. As a result, a volume based and structurally independent mean thickness estimation method is presented by (Hildebrand & Ruegsegger, 1997)<sup>16</sup>. Based on this approach, local thickness at a given point within the structure is defined as the diameter of the maximal sphere which can be fitted completely inside the structure. In this project, a discrete interpretation of this method will be applied to measure the mean cortical thickness of IPD, PSP and HC subjects using the Visualization Toolkit (VTK). VTK is an open source and widely used software for image processing and 3D graphics which supports extensive visualization algorithms such as vector, tensor, texture and volumetric based methods<sup>17</sup>. This cross platform software

which is primarily built on C++ libraries has several interfaces with high level dynamic programming languages such as Python<sup>18</sup>.

Overall, this paper discusses the implementation of the discrete version of the method proposed by (Hildebrand & Ruegsegger, 1997) on cortical T1-weighted MRI datasets of PSP, IPD and HC subjects. Statistical methods such as analysis of variance (ANOVA) will be applied on the results to elucidate any significant inter group differences. The article is then concluded with a discussion section.

## **II. Materials and Methods**

### **II.I) Dataset**

Multi-spectral MRI datasets from 76 IPD patients, 22 PSP patients, and 40 age-matched healthy control subjects acquired at the University Medical Center Hamburg-Eppendorf, Germany, using a 3T Siemens Skyra MR scanner are available for this research project. The dataset includes T1-weighted preregistered images using the Montreal Neurological Institute (MNI) atlas in the Neuroimaging Informatics Technology Initiative (NIFTI) format. In detail, affine registration of the atlas was conducted using a block matching approach for pre alignment. Moreover, the resulting deformation field was then used to wrap 21 sub cortical regions as defined in the MNI space to each subject by using a nearest neighbor interpolation. Demographic information of this dataset is currently unavailable.

### **II.II) System specifications**

This project uses VTK version 6 on Python version 2.7.11. All operations are done in Mac OS x El Capitan version 10.11.4. Additional hardware specifications are included in Appendix 2.

### **II.III) Background**

The paper by (Hildebrand & Ruegsegger, 1997) presents a structurally independent mean thickness measurement method. Based on their approach, a volume based thickness is estimated by the fitting of maximal spheres to every point in the structure. This continuous method needs to be readjusted to be used in discrete images. In this context, segmented images are defined by binary voxels where, the voxel is either segmented or not segmented and therefor is part of the background. In order to translate the aforementioned technic into it's discrete form, the distance map needs to be calculated. The distance map, which is defined by assigning the square Euclidian distance from all segmented voxels to the nearest non segmented voxel, is derived by the distance transform. This interpretation is equal to the radius of the largest sphere centered at that point which still completely is within the structure.

## II.IV) Preprocessing

Before applying the discrete version of the method proposed by (Hildebrand & Ruegsegger, 1997), we first need to take some pre processing measures. The first step is to read the NIFTI images by using the implemented NIFTI reader for VTK in Python. As an additional aid, we have used a b-ware called ITK-SNAP<sup>19</sup> to pre visualize the images. ITK-SNAP is primarily used for segmentation in 3D medical image however, it can be used to analyze image intensities as well as other important image information. Figure 2.1 depicts the three dimensional visualization of one of the healthy controls using ITK -SNAP. Based on visual inspection, the left and right cortex is found to have intensity values of 2 and 13, respectively.

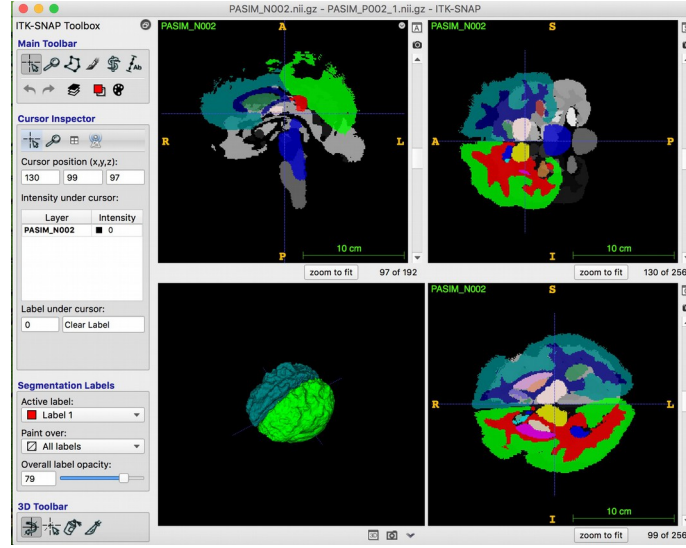


Figure 2.1. 3D Depiction of Subject 002 using ITK SNAP

In Figure 2.1 the green colored and blue cortex are the left (Intensity = 2) and right cortex (Intensity =13), respectively. Therefore, as the next preprocessing step, intensity thresholding was performed based on the values of 2 and 13 which discards all non 13 and 2 intensities, effectively segmenting the cortex and turning the multi intensity image into two binary images. Figures 2.2 and 2.3 depict the original and segmented image before and after thresholding, respectively.

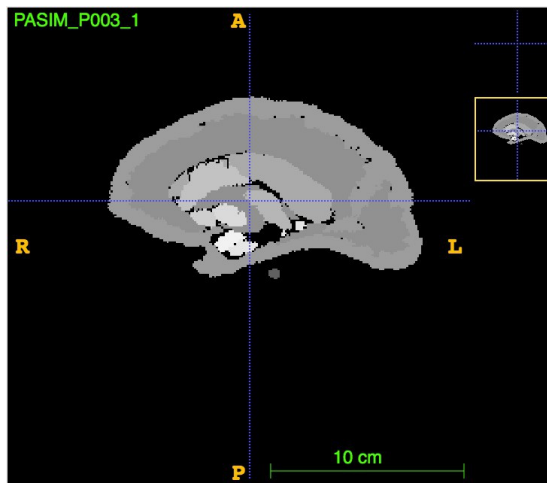


Figure 2.2. Original NIFTI image before any thresholding



Figure 2.3. Thresholded (Segmented) image of Figure 2.2

As the last preprocessing step, the Euclidian distance transform is applied to the segmented image. In detail, this transform assigns each voxel the square Euclidian distance to the nearest non segmented area. The algorithm behind this transform (Saito's Algorithm<sup>20</sup>) is highly efficient for relatively small data, however, since the images in this project are large (256 by 256 by 192) we need to use the alternative version of this transform namely, the cached Saito algorithm which is also implemented for VTK.

## II.V) Mean Thickness Estimation

The algorithm uses three nested for loops for the three image dimensions. In detail, the algorithm checks if the currently observed voxel is segmented or non segmented. If the voxel is not segmented the next voxel is observed. If a segmented voxel is found, then the algorithm defines a window around the center voxel with a specific radius. The radius is defined as the square root of the Euclidian distance of the center voxel. The algorithm then enters a second three layer nested for loop. Inside this window, the square root value of each voxel is compared to the square root of the Euclidian distance of the center voxel. If the center voxel has a higher value compared to the current voxel inside the secondary window, then that voxel will be assigned the value of the center voxel. Otherwise the voxel is left unchanged. This process is iteratively continued until all voxels are upgraded. The local thickness is then defined as the radius times two. In order to account for the effect of noise, we have decided to exclude voxels with values (thickness) less than 1mm. In this context, we have defined the thickness as following:

$$\text{Mean} = \text{Total\_sum} / \text{EffectiveSegmentedVoxels}$$

Here, Total\_sum is the summation of all the voxel values (less than 1mm voxels are excluded from Total sum) and EffectiveSegmentedVoxels is the number of all the non zero voxels which have values bigger than 1mm. Moreover, we defined the overall mean thickness as the following:

$$\text{Overall Thickness} = (\text{Left Cortex mean} + \text{Right Cortex Mean}) / 2$$

This approach is perfectly aligned with the continuous version presented by (Hildebrand & Ruegsegger, 1997). The pseudo code of the implemented method is as follows:

1. Iterate through Image
2. Look at Voxel (X,Y,Z)
3. If (X,Y,Z) = D is segmented go to 4; else go to 1
4. Define window with radius D
5. Iterate in window
6. If square root of ( $I^2 + J^2 + K^2$ ) is less or equal to D go to 7; else go to 5
7. If D at that point is nonzero and the square root of Euclidian distance at that point ( $D^*$ ) is less or equal to D
8. Assign D to  $D^*$
9. Repeat

The output of the above mentioned algorithm is depicted in figure 2.4 where the warmer colors indicate thicker areas.

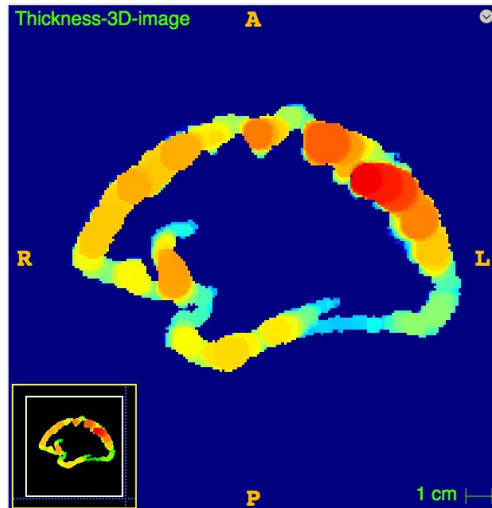


Figure 2.4. Final thickness image of Figure 2.3

### III. Results & Analysis

#### III.I) Results

After applying the above mentioned method, the mean thickness measurements of all the subjects are calculated. The individual results for the healthy controls are depicted in table 3.1. Moreover, PSP and IPD measurements are depicted in tables 3.2 and 3.3, respectively. In all the tables in this section, L-Mean thickness, R-Mean thickness and

O-Mean thickness signify left, right and overall mean measurements. All values are in millimeters.

Table 3.1. Mean cortical thickness measurements of healthy controls

Subject ID	L-Mean thickness	R-Mean thickness	O-Mean thickness
PASIM_N002	11.5737454768	11.6605630346	11.6171542557
PASIM_N003	12.0292832991	12.1045778844	12.0669305917
PASIM_N004	11.4468689917	11.7009573749	11.5739131833
PASIM_N005	11.3771640337	10.9381085146	11.1576362742
PASIM_N006	11.6223777957	11.5344066601	11.5783922279
PASIM_N007	11.7584353501	11.9865633204	11.8724993352
PASIM_N008	12.635622382	12.4891954208	12.5624089014
PASIM_N009	11.7279355839	11.6434763675	11.6857059757
PASIM_N010	12.4213026312	12.6439371572	12.5326198942
PASIM_N011	11.7258909704	11.762996051	11.7444435107
PASIM_N012	11.835533869	11.6755569226	11.7555453958
PASIM_N013	12.485840797	12.5783417887	12.5320912928
PASIM_N014	11.871119776	12.0844731813	11.9777964786
PASIM_N015	12.1576400021	12.0842524592	12.1209462307
PASIM_N016	11.8591723264	11.6616834531	11.7604278897
PASIM_N017	12.2049641149	12.2265511365	12.2157576257
PASIM_N018	12.5418935385	12.2302665831	12.3860800608
PASIM_N019	12.1306023194	12.0203400348	12.0754711771
PASIM_N020	11.6892857139	11.6818932704	11.6855894922
PASIM_N021	12.0862413184	11.903084546	11.9946629322
PASIM_N022	12.2718241776	12.1104940946	12.1911591361
PASIM_N023	11.9795183998	11.8108516844	11.8951850421
PASIM_N024	12.5366994944	12.201444984	12.3690722392
PASIM_N025	11.3046337097	11.2921039746	11.2983688421
PASIM_N026	11.3463329289	11.4308560322	11.3885944806
PASIM_N027	12.6296358493	12.2056087109	12.4176222801
PASIM_N028	12.0709588103	12.0048748584	12.0379168343
PASIM_N029	12.2123663632	11.9701232712	12.0912448172
PASIM_N030	12.3075210354	11.9804751537	12.1439980945
PASIM_N031	12.1225295249	11.7077501747	11.9151398498

PASIM_N032	12.5656817878	12.0227243576	12.2942030727
PASIM_N033	11.531537308	11.3835644883	11.4575508982
PASIM_N034	12.4644169454	12.0175391745	12.2409780599
PASIM_N035	11.8867659673	11.5712830274	11.7290244974
PASIM_N036	11.8570062247	11.8276421929	11.8423242088
PASIM_N037	11.8782239037	11.5372692873	11.7077465955
PASIM_N038	12.1490342983	11.9469162749	12.0479752866
PASIM_N039	11.8853354401	11.4499354399	11.66763544
PASIM_N040	11.5092060838	11.4460845403	11.4776453121
PASIM_N041	12.3215464308	11.9990632346	12.1603048327

Table 3.2. Mean cortical thickness measurements of PSP subjects

Subject ID	L-Mean thickness	R-Mean thickness	O-Mean thickness
PASIM_P003	11.2218294186	11.2418923274	11.231860873
PASIM_P004	12.1839792066	11.8059597292	11.9949694679
PASIM_P009	11.6326278329	11.5941008022	11.6133643176
PASIM_P010	11.07660496	10.8118233595	10.9442141598
PASIM_P011	12.1214644234	11.4775952878	11.7995298556
PASIM_P014	11.4560134652	11.4965240785	11.4762687719
PASIM_P028	11.6060109598	11.7154141811	11.6607125705
PASIM_P033	12.1526156816	11.9223008292	12.0374582554
PASIM_P041	11.2203523658	11.4756365368	11.3479944513
PASIM_P050	12.1043773425	12.2787793041	12.1915783233
PASIM_P051	12.6514792894	12.497466279	12.5744727842
PASIM_P056	11.5770426399	11.4961962175	11.5366194287
PASIM_P093	12.674711603	12.2176230577	12.4461673304
PASIM_P098	11.2942729826	10.9471837588	11.1207283707
PASIM_P105	11.7818052199	11.3721105893	11.5769579046
PASIM_P106	12.6823757615	12.4078086982	12.5450922298
PASIM_P107	12.3585745956	12.2243474135	12.2914610046
PASIM_P108	11.6017087085	11.3884361499	11.4950724292
PASIM_P109	11.9036762226	11.7850735488	11.8443748857
PASIM_P110	11.8724852648	11.829027261	11.8507562629
PASIM_P111	11.2464369701	11.0554130975	11.1509250338
PASIM_P112	11.5822459446	11.496872765	11.5395593548



Table 3.3. Mean cortical thickness measurements of IPD subjects

Subject ID	L-Mean thickness	R-Mean thickness	O-Mean thickness
PASIM_P002_1	11.8973	11.6330811029	11.7651905515
PASIM_P005_1	11.9447	11.8763482049	11.9105241024
PASIM_P006_1	12.2832	12.3756502683	12.3294251342
PASIM_P007_1	12.3583	12.2477584876	12.3030292438
PASIM_P008_1	11.5948	11.6013564592	11.5980782296
PASIM_P012_1	12.0748	11.836633368	11.955716684
PASIM_P013_1	12.4295	12.2063158788	12.3179079394
PASIM_P016_1	11.0182	11.4511044372	11.2346522186
PASIM_P019_1	11.1648100998	11.2881068934	11.2264584966
PASIM_P020_1	12.1748714585	11.7508920356	11.962881747
PASIM_P021_1	11.4792981763	11.4250876648	11.4521929206
PASIM_P023_1	11.9795798522	12.4010330214	12.1903064368
PASIM_P024_1	11.464709633	11.4757865556	11.4702480943
PASIM_P026_1	11.4978580288	11.8763884033	11.6871232161
PASIM_P029_1	11.8374896571	11.7271440474	11.7823168523
PASIM_P031_1	11.8128397253	11.9852788191	11.8990592722
PASIM_P032_1	12.1214051993	12.0902831116	12.1058441555
PASIM_P035_1	11.6225045022	11.5313232797	11.5769138909
PASIM_P036_1	12.1158499478	12.0783247915	12.0970873696
PASIM_P038_1	12.0789544559	12.0802323966	12.0795934262
PASIM_P039_1	12.4713533325	11.7939091766	12.1326312545
PASIM_P040_1	12.4655595491	12.5582447989	12.511902174
PASIM_P043_1	11.376349619	11.4277534816	11.4020515503
PASIM_P044_1	11.3626417961	11.2914207804	11.3270312882
PASIM_P045_1	12.1498882774	12.1279998356	12.1389440565
PASIM_P046_1	12.1753011902	12.302224796	12.2387629931
PASIM_P047_1	12.1719042637	11.9872135021	12.0795588829
PASIM_P048_1	11.857712522	11.469516611	11.6636145665
PASIM_P049_1	11.571316795	11.8606755426	11.7159961688
PASIM_P053_1	12.4194374317	12.204680824	12.3120591279
PASIM_P057_1	11.6183368234	11.416456393	11.5173966082

PASIM_P059_1	12.2634571383	11.4124876666	11.8379724024
PASIM_P063_1	12.0896078372	12.1700001122	12.1298039747
PASIM_P064_1	12.1583139876	12.4254290109	12.2918714992
PASIM_P065_1	12.4340195225	12.2686019239	12.3513107232
PASIM_P066_1	11.4715880686	11.457672397	11.4646302328
PASIM_P067_1	11.8081530207	11.6113476252	11.709750323
PASIM_P068_1	12.3560847238	12.1705100598	12.2632973918
PASIM_P069_1	11.9781084885	12.0599055002	12.0190069944
PASIM_P070_1	12.1438236194	11.6671388654	11.9054812424
PASIM_P071_1	11.9237689496	11.7029973975	11.8133831736
PASIM_P078_1	12.9351208436	12.5942734997	12.7646971716
PASIM_P079_1	12.2440180783	11.729264082	11.9866410802
PASIM_P080_1	11.8472647587	11.9276568907	11.8874608247
PASIM_P085_1	12.3980775902	12.2983794046	12.3482284974
PASIM_P086_1	11.8270226909	11.6224782567	11.7247504738
PASIM_P088_1	11.1160949923	10.9978606899	11.0569778411
PASIM_P089_1	12.5120396406	12.1013046626	12.3066721516
PASIM_P090_1	11.6585429387	11.2758015605	11.4671722496
PASIM_P092_1	12.5845223681	12.2742781434	12.4294002558
PASIM_P094_1	11.6435567373	11.6442073477	11.6438820425
PASIM_P095_1	12.1291309878	11.9334099577	12.0312704728
PASIM_P096_1	11.6311628472	11.5630644393	11.5971136433
PASIM_P097_1	11.2241566444	10.8549704463	11.0395635453
PASIM_P102_1	12.35595626	11.9875172297	12.1717367448
PASIM_P103_1	12.0411323284	11.6643586958	11.8527455121
PASIM_P201	11.7033517285	11.5301419683	11.6167468484
PASIM_P202	11.7052101775	11.5547231185	11.629966648
PASIM_P203	12.2164035887	11.8959068864	12.0561552376
PASIM_P204	11.9953522144	11.6249173854	11.8101347999
PASIM_P205	12.5689898948	12.5888792041	12.5789345495
PASIM_P206	11.770603561	11.7753536643	11.7729786127
PASIM_P207	11.8401473732	11.3061396346	11.5731435039
PASIM_P208	12.3952631034	12.1864694931	12.2908662983
PASIM_P209	11.4703056421	10.9442105717	11.2072581069
PASIM_P210	12.7164568985	12.7269204441	12.7216886713

PASIM_P211	11.3168627598	11.178799214	11.2478309869
PASIM_P212	11.940131761	11.6151026497	11.7776172054
PASIM_P213	11.6182752369	11.5289665187	11.5736208778
PASIM_P214	11.7794406217	11.684617246	11.7320289338
PASIM_P215	12.00649233	11.6660535702	11.8362729501
PASIM_P216	12.1502987589	11.6616622433	11.9059805011
PASIM_P217	10.7714679667	10.8607814774	10.816124722
PASIM_P218	11.9907004988	11.5714474779	11.7810739884
PASIM_P219	12.4125676872	11.8430593539	12.1278135205
PASIM_P220	11.5307288805	11.394818071	11.4627734757

### III.II) Statistical Analysis

Average values of the mean thickness along with standard deviation for the study groups is shown in Table 3.4. Furthermore, one way analysis of variance (ANOVA) was conducted using SPSS<sup>21</sup> for all the binary cases to inspect any inter group differences. ANOVA results for HC vs. IPD, HC vs. PSP and PSP vs. IPD are shown in Table 3.5. Bonferoni correction was used for multiple comparison. Overall, statistical analysis show no significant inter group differences ( $p > 0.05$ ). Additional information regarding the statistical analysis are included in Appendix A.

Table 3.4. Mean and standard deviation of the measured thickness values for each group

Metric/Subject Group	HC	PSP	IPD
Mean	11.9317440636	11.7395517303	11.8631359152
Standard Deviation	0.347323472101	0.455624408403	0.397290881766

Table 3.5. Significance levels between groups for structure measures

Groups/Brain Region	Left Cortex	Right Cortex	Whole Cortex
HC vs. IPD	$p > 0.99$	$p > 0.99$	$p > 0.99$
HC vs. PSP	$p = 0.323$	$p = 0.187$	$p = 0.213$
PSP vs. IPD	$p = 0.738$	$p = 0.586$	$p = 0.606$

The stem and leaf plot of the whole, left and right cortex are shown in figures 3.1, 3.2 and 3.3 respectively.

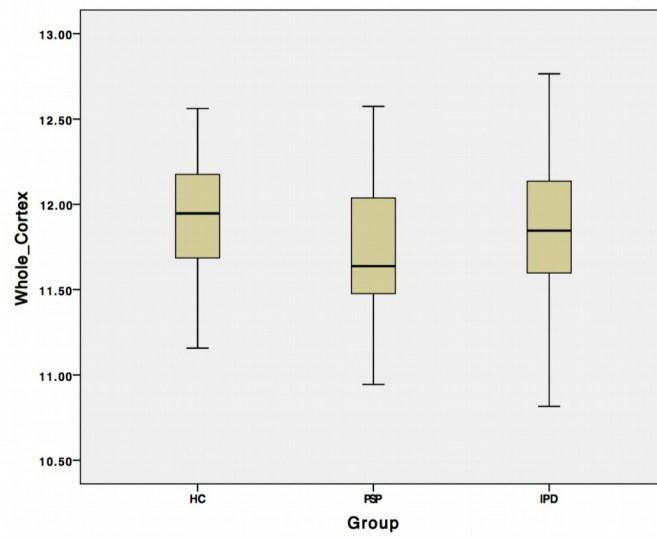


Figure 3.1. Stem and leaf plot for the whole cortex

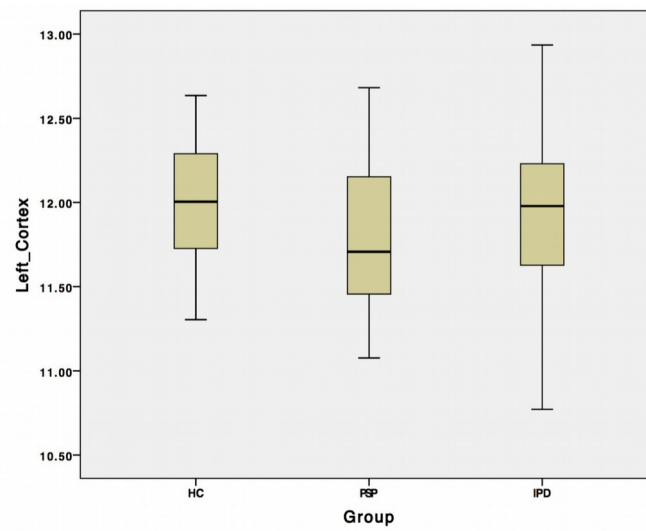


Figure 3.2. Stem and leaf plot for the left cortex

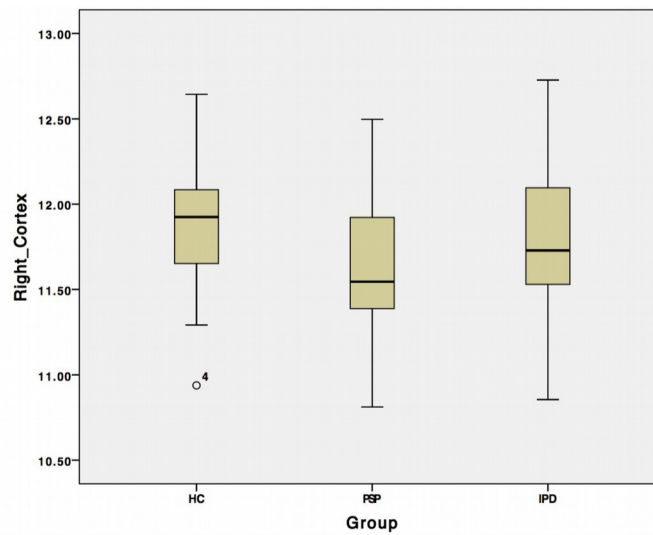


Figure 3.3. Stem and leaf plot for the right cortex

## IV. Discussion

In this paper, the structurally independent mean thickness measurement method proposed by (Hildebrand & Ruegsegger., 1997) was implemented on T1-weighted preregistered images of different Parkinson's disease (PD) syndromes and healthy controls. Based on this approach, we calculated the mean cortical thickness of PSP, IPD and healthy controls over the left, right and the whole cortex and performed statistical analysis, namely ANOVA on them. Based on the obtained results, no significant differences were found between any of the studied groups. However, the results are completely reasonable with respect to anatomical information. For instance, sensory areas tend to be among the thinnest structures in the cortex. Our generated 3D model of the brain after processing shows that these areas appear to be indeed thinner relative to other brain regions. Moreover, in order to validate our algorithm a cube with known thickness was generated. The algorithm produced favorable results once it was applied to this phantom.

One important aspect of this study is that the obtained cortical thickness values are significantly higher than what is described in the literature. While the mean cortical thickness value is about 2.5 millimeters, our results show that for each group they are larger than 11 millimeters. This discrepancy may be explained in two ways. First of all, the dataset that we used was not specifically generated for the purpose of this study. In fact, as it is described in the materials and methods section, they were primarily registered to be used in studies related to sub cortical structures. Consequently, cortical voxels appear bigger than what they actually are and therefore the thickness values inherently tend to be larger. Secondly, the formula that we used for mean thickness measurement blindly calculates the thickness over the entire cortex without accounting for region specific thickness weightings. Different weighting schemes, which assign less weight to thinner regions should be implemented to refine the results. As a future direction, we hope that by addressing the two above mentioned limitations, we will find significant inter group differences. As an additional future direction, we want to implement a region specific mean thickness estimator. This improvement upon this pre established framework is more sensible than whole cortex mean thickness calculations because many neurodegenerative illnesses such as Parkinson's disease exhibit region specific cortical thinning. These constrained cortical thinning may be used as disease specific biomarkers.

The following study has several limitations. First, the programming language used in this research (Python) inherently suffers from poor performance compared to C++ which is the standard software for image processing related projects. Unlike Python, C++ uses memory more efficiently by giving the programmer explicit control over memory allocation. In fact, the expansive access that C++ provides is crucial for CPU cache which is an important performance factor. Furthermore, the performance deficiency of python was evident when we compared it to C++ by using the same algorithm in both languages for thickness measurement. While the python program, in it's most efficient form, took about 7 minutes to produce the thickness value, C++ was able to do the same task in less than a minute. Secondly, similar studies to this project, generally use the Insight segmentation and registration toolkit (ITK) over VTK. Due to the iterative and computationally expensive nature of the implemented algorithm, the use of ITK in C++ (along with the extensive use of C++ pointers) will certainly improve performance.

In conclusion, the implemented algorithm based on the method of (Hildebrand & Ruegsegger, 1997) shows promising initial results. We are hoping that by improving this framework, significant inter group differences will be found.

## V. References

1. Mhyre, T. R., Boyd, J. T., Hamill, R. W. & Maguire-Zeiss, K. A. *Protein Aggregation and Fibrillogenesis in Cerebral and Systemic Amyloid Disease. Sub-cellular biochemistry* **65**, (2012).
2. FEARNLEY, J. M. & LEES, A. J. Ageing and Parkinson's Disease: Substantia Nigra Regional Selectivity. *Brain* **114**, 2283–2301 (1991).
3. Gattellaro, G. *et al.* White matter involvement in idiopathic Parkinson disease: A diffusion tensor imaging study. *Am. J. Neuroradiol.* **30**, 1222–1226 (2009).
4. Tambasco, N. *et al.* Magnetization transfer changes of grey and white matter in Parkinson's disease. *Neuroradiology* **45**, 224–30 (2003).
5. Morelli, M. *et al.* Accuracy of magnetic resonance parkinsonism index for differentiation of progressive supranuclear palsy from probable or possible Parkinson disease. *Mov. Disord.* **26**, 527–533 (2011).
6. Pyatigorskaya, N., Gallea, C., Garcia-Lorenzo, D., Vidailhet, M. & Lehericy, S. A review of the use of magnetic resonance imaging in Parkinson's disease. *Ther. Adv. Neurol. Disord.* **7**, 206–220 (2013).
7. Zhu, M.-W., Liu, J., Arzberger, T., Wang, L.-N. & Wang, Z.-F. Typical or atypical progressive supranuclear palsy: a comparative clinicopathologic study of three Chinese cases. *Int J Clin Exp Pathol* **8**, 867–874 (2015).
8. Rolheiser, T. M. *et al.* Diffusion tensor imaging and olfactory identification testing in early-stage Parkinson's disease. *J. Neurol.* **258**, 1254–1260 (2011).
9. Hughes, A. J., Daniel, S. E., Kilford, L. & Lees, A. J. Accuracy of clinical diagnosis of idiopathic Parkinson's disease : a clinico-pathological study of 100 cases. 181–184 (1992). doi:10.1136/jnp.55.3.181
10. Ene, M. Neural network-based approach to discriminate healthy people from those with Parkinson's disease. *Ann. Univ. Craiova, Math. Comp. Sci. Ser.* **35**, 112–116 (2008).
11. Messina, D. *et al.* Patterns of brain atrophy in Parkinson's disease, progressive supranuclear palsy and multiple system atrophy. *Parkinsonism Relat. Disord.* **17**, 172–176 (2011).

12. Tang, C. C. *et al.* Differential diagnosis of parkinsonism: a metabolic imaging study using pattern analysis. *Lancet Neurol.* **9**, 149–158 (2010).
13. Forkert, N. D. *et al.* Image-based classification of parkinsonian syndromes using T2'-atlases. *Stud. Health Technol. Inform.* **169**, 465–469 (2011).
14. Gupta, D., Saini, J., Kesavadas, C., Sarma, P. S. & Kishore, A. Utility of susceptibility-weighted MRI in differentiating Parkinson's disease and atypical parkinsonism. *Neuroradiology* **52**, 1087–1094 (2010).
15. Fischl, B. & Dale, A. M. Measuring the thickness of the human cerebral cortex from magnetic resonance images. *Proc Natl Acad Sci U S A* **97**, 11050–11055 (2000).
16. Hildebrand, T. & Rügsegger, P. A new method for the model-independent assessment of thickness in three-dimensional images. *J. Microsc.* **185**, 67–75 (1997).
17. VTK - The Visualization Toolkit. Available at: <http://www.vtk.org/>. (Accessed: 11th April 2016)
18. Welcome to Python.org. Available at: <https://www.python.org/>. (Accessed: 11th April 2016)
19. Gerig, G. HomePage. Available at: <http://www.itksnap.org/pmwiki/pmwiki.php>. (Accessed: 11th April 2016)
20. VTK: vtkImageEuclideanDistance Class Reference. Available at: <http://www.vtk.org/doc/nightly/html/classvtkImageEuclideanDistance.html>. (Accessed: 12th April 2016)
21. IBM SPSS - IBM Analytics. Available at: <http://www.ibm.com/analytics/us/en/technology/spss/>. (Accessed: 20th April 2016)